Mathematical modelling of temperature distribution during CO_2 laser irradiation of glass

A. Helebrant, C. Buerhop & R. Weißmann

Universität Erlangen-Nürnberg, Institut für Werkstoffwissenschaften III (Glas und Keramik), Martensstr. 5, W-8520 Erlangen, Germany

Manuscript received 21 December 1992
Revision received 25 January 1993

The irradiation of glass using a CO_2 laser causes a local temperature rise which can be used for local heat treatments, e.g. polishing, cutting. The temperature distribution is described generally by the heat diffusion equations. If the laser beam radius is much larger than the material thickness, the two dimensional problem can be replaced with a one dimensional solution. For the simulation it is necessary to take the strong temperature dependence of the thermal conductivity and the specific heat of the glass into account and also the boundary conditions. The boundary conditions only become important at irradiation times longer than 2 s; then the glass properties play a more important role. Here, the thermal conductivity influences the temperature most significantly, due to the strong effect of heat transfer by radiation in glass at high temperatures. This large thermal conductivity results in a rather even temperature distribution in the glass.

The absorption of intense ir-radiation from a CO_2 laser beam causes local temperature rises and consequently induces thermal stresses. If the induced stress exceeds a certain critical value, the glass fractures catastrophically. By controlling the stress and the crack propagation, this effect can be ingeniously used for the rapid cutting of glass. By preheating the glass, the critical stresses are minimised and local heat treatments based on annealing, melting, and evaporation effects can be carried out using CO_2 laser radiation.[1]

For successful laser heat treatment, the local and temporal temperature distribution is of great importance. The temperature depends on the laser parameters: laser power, laser beam intensity, feed speed, irradiated area, time of interaction, and intensity distribution; and on the glass properties: predominantly thermal conductivity and specific heat.

Basic solutions of the heat conduction equation are described by Carslaw & Jaeger.[2] A survey of analytical solutions for the interaction of laser radiation with a material is presented by Zscherpe.[3] A solution of the thermal influence of a moving laser beam on metals is derived by Geissler & Bergmann.[4]

If glass is the target material, the situation is more complex than that for metals. The main reasons are:

1. The thermal properties of glass are strongly dependent on temperature, e.g. the heat transfer increases due to radiation at high temperatures.
2. Heat losses due to radiation become important at temperatures above 400°C, because the emissivity of a glass surface is higher than that of a metal surface. That is, the boundary condition for the irradiated surface does not behave linearly with temperature.

A numerical solution is therefore necessary to solve the heat conduction equation.

The aims of this paper are to show how strongly the temperature distribution varies with the temperature dependent glass properties, and how it is affected by various boundary conditions. The modelling is carried out for parallel sided flat glass, whose properties are given in Table 1.

Table 1. *Float glass properties at room temperature*

	Float glass
R	$\approx 0{\cdot}2$
$1/\alpha$	1–10 μm
k	$1{\cdot}1\ \mathrm{Jm^{-1}\,s^{-1}\,K^{-1}}$
c_p	$780\ \mathrm{Jkg^{-1}\,K^{-1}}$

Notation

- α absorption coefficient, $\mathrm{cm^{-1}}$
- d_d heat diffusion length, m
- T temperature, K
- t time of interaction, s
- r distance from laser beam centre, m
- r_m laser beam radius, m
- z distance from irradiated glass surface, m
- z_m glass thickness, m
- k thermal conductivity, $\mathrm{Wm^{-1}\,K^{-1}}$
- c_p specific heat, $\mathrm{Jkg^{-1}\,K^{-1}}$
- ρ glass density, $\mathrm{kgm^{-3}}$
- I_0 laser intensity, $\mathrm{Wm^{-2}}$
- R glass reflectivity
- σ Boltzmann constant, $5{\cdot}667\times10^{-8}\ \mathrm{Wm^{-2}\,K^{-4}}$

ε glass surface emissivity,
h heat convection coefficient, $Wm^{-2} K^{-1}$
T_c temperature of coolant in contact with glass, K
T_g transformation temperature, K
T_0 temperature of glass at the beginning of interaction, K
κ average heat diffusivity of glass, $m^2 s^{-1}$

Heat conduction equation

Assuming cylindrical symmetry, two forms of the general heat conduction equation are derived:

volume heat source

$$\rho c_p \frac{\partial T}{\partial t} = \left[\frac{k}{r} + \frac{\partial k}{\partial r}\right]\frac{\partial T}{\partial r} + \frac{\partial k}{\partial z}\frac{\partial T}{\partial z} + k\left[\frac{\partial^2 T}{\partial r^2} + \frac{\partial^2 T}{\partial z^2}\right] + \frac{dI}{dz} \quad (1)$$

surface heat source

(laser beam intensity is included in the boundary condition on the irradiated surface)

$$\rho c_p \frac{\partial T}{\partial t} = \left[\frac{k}{r} + \frac{\partial k}{\partial r}\right]\frac{\partial T}{\partial r} + \frac{\partial k}{\partial z}\frac{\partial T}{\partial z} + k\left[\frac{\partial^2 T}{\partial r^2} + \frac{\partial^2 T}{\partial z^2}\right] \quad (2)$$

If the absorption depth $1/\alpha$ is less than the heat diffusion length, d_d

$$1/\alpha \ll d_d \approx \sqrt{4\kappa t} \quad (3)$$

the thermal interaction of the laser radiation with the target can be described as surface heat source.

As shown in Table 1, the glass absorption coefficient α of the CO_2 laser wavelength ($\lambda = 10{\cdot}6\ \mu m$)[5,6] is so high that the energy is deposited within a very small surface layer.

With $\kappa \approx 0{\cdot}5\text{–}1 \times 10^{-6}\ m^2/s$ and an assumed interaction time $t = 0{\cdot}25$ s, the temperature diffusion length is $d_d \approx 7{\cdot}0 \times 10^{-4}$ m to $1{\cdot}0 \times 10^{-3}$ m according to Equation (3). Because d_d is much larger than the absorption depth of the CO_2 laser radiation in glass, the CO_2 laser beam may be considered as a surface heat source.

Boundary conditions

The following sections discuss the relevant boundary conditions for glass—laser beam—interaction.

Beam axis direction.

Front surface

$$-k\left[\frac{\partial T}{\partial z}\right]_{z=0} = I(r,t) - \sigma\varepsilon(T^4_{z=0} - T^4_c) - h(T_{z=0} - T_c) \quad (4)$$

with $I = I_0\,(1 - R)$.

The first term on the right side of Equation (4) represents the heat source, the second term the radiation loss and the third the convection loss.

Two common laser beam geometries will be discussed, a rectangular intensity distribution ($I = I_0$ for $r \leqslant r_m$; $I = 0$ for $r > r_m$) and a Gaussian intensity distribution ($I = I_0 \exp(-r^2/r_m^2)$).

Back surface

$$k\left[\frac{\partial T}{\partial z}\right]_{z=z_m} = -\sigma\varepsilon(T^4_{z=z_m} - T^4_c) - h(T_{z=z_m} - T_c) \quad (5)$$

If the glass sample is perfectly insulated at the rear side, convection and radiation losses are negligible, then it follows

$$\left[\frac{\partial T}{\partial z}\right]_{z=z_m} = 0 \quad (6)$$

If the glass thickness is larger than the heat diffusion length d_d ($z_m \gg \sqrt{4\kappa t}$) and convection and radiation losses can be neglected or when the radiation and convection losses are equal to the heat flux at $z = z_m$, then

$$T_{z_m} = T_0 \quad (7)$$

Radial direction. For the symmetrical intensity distribution

$$\left[\frac{\partial T}{\partial r}\right]_{r=0} = 0 \quad (8)$$

When the glass sample is radially much larger than the beam radius

$$T_{r\to\infty} = T_0 \quad (9)$$

As $r \to \infty$, $r \gg \sqrt{4\kappa t}$.

Temperature dependence of the thermal properties

Thermal conductivity. Heat is conducted in glasses by lattice vibrations (phonon conductivity) and radiation (photon conductivity). Usually, the radiation is neglected, but it becomes important at high temperatures because it is proportional to the fourth power of temperature.

The thermal conductivity due to lattice vibrations is taken as constant ($T_1 = 298$ K, $T_2 = 973$ K) and temperature dependent. Also, heat transfer by radiation is considered.

Two constant values were used, $k_1 = 1{\cdot}1\ Wm^{-1} K^{-1}$ for room temperature (298 K) and $k_2 = 2{\cdot}1\ Wm^{-1} K^{-1}$ for 700°C (973 K).

The temperature dependence of the thermal conductivity k without additional heat transfer by radiation is fitted by a sixth degree polynomial.

Assuming a limiting k value of $2{\cdot}1\ Wm^{-1} K^{-1}$:

$$\begin{aligned} k(T) = {} & 1{\cdot}098503 + 3{\cdot}5 \times 10^{-5}(T-273) \\ & + 8{\cdot}015397 \times 10^{-6}(T-273)^2 \\ & - 1{\cdot}494571 \times 10^{-8}(T-273)^3 \\ & + 1{\cdot}139537 \times 10^{-11}(T-273)^4 \\ & - 4{\cdot}016636 \times 10^{-15}(T-273)^5 \\ & + 5{\cdot}412311 \times 10^{-19}(T-273)^6 \end{aligned} \quad (10)$$

Considering heat transfer by radiation the temperature dependence of the thermal conductivity k can be

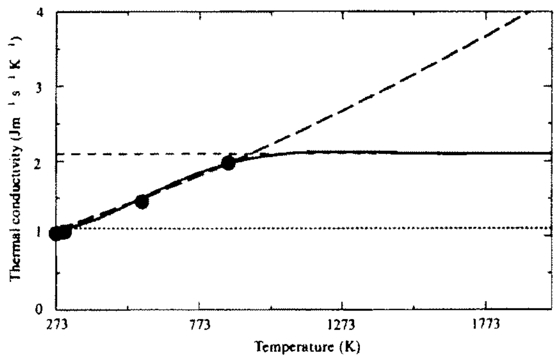

Figure 1. *Temperature dependence of the thermal conductivity of float glass*
● k from Ref. 6 ----- $k=k_2$ ——— $k=f(T^4)$
------ $k=k_1$ ——— $k=f(T)$

determined from the glass composition according to Ammar *et al.*[7] for various temperatures: 0, 30, 300, 600°C. These values are fitted by a second degree polynomial to simulate heat transfer by radiation

$$k(T^4)=1\cdot084381+0\cdot001312(T-273)+2\cdot778335\times10^{-7}(T-273)^2 \quad (11)$$

The different dependences of the thermal conductivity are presented in Figure 1.

Specific heat. The specific heat can be considered as constant, temperature dependent, or temperature dependent with an additional nonlinear increase at T_g. On passing through the glass transition to the liquid state, the specific heat generally increases. The increased specific heat reflects the increase in configurational entropy which becomes possible in the liquid state, in which the time for molecular rearrangement is short with respect to the experimental time scale.

According to Sharp, the average value of c_p for temperature interval 273–1573 K is 1222 $Jkg^{-1}K^{-1}$.[8]

The temperature dependence for the specific heat is given by Sharp[8]

$$c_p(T)=\frac{\left[\begin{array}{l}7\cdot519\times10^{-7}(T-273)^2\\ \quad+10\cdot3\times10^{-4}(T-273)+0\cdot176\end{array}\right]}{(0\cdot00146(T-273)+1)^2}4178 \quad (12)$$

The jump of c_p at the transformation temperature is simulated by

$$c_p=\frac{\left[\begin{array}{l}7\cdot519\times10^{-7}(T-273)^2\\ \quad+10\cdot3\times10^{-4}(T-273)+0\cdot176\end{array}\right]}{(0\cdot00146(T-273)+1)^2}4178 \quad (13)$$

for $T_g\leqslant803$ K, and

$$c_p=\frac{\left[\begin{array}{l}7\cdot519\times10^{-7}(T-273)^2\\ \quad+10\cdot3\times10^{-4}(T-273)+0\cdot176\end{array}\right]}{(0\cdot00146(T-273)+1)^2}4178+122\cdot2 \quad (14)$$

for $T_g\geqslant803$ K.

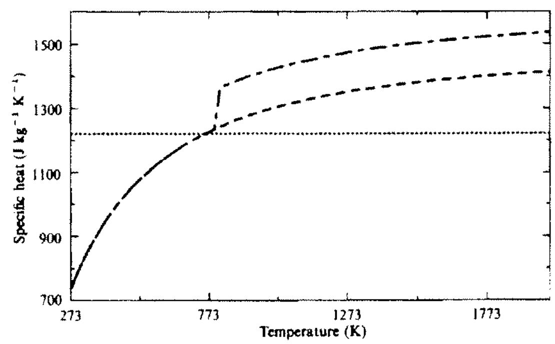

Figure 2. *Temperature dependence of the specific heat of float glass*
------ c_p = const — — — $c_p=f(T)$ with jump at T_g
----- $c_p=f(T)$

These dependences are depicted in Figure 2.

The temperature dependence of the glass density is neglected in this work.

Results and discussion

Equation (2) is solved using the finite difference method. For a stable solution the step size of the time interval is adjusted to the spatial step size dz in the axial direction as follows

$$dt\leqslant\frac{dz^2}{4k/\rho c_p} \quad (15)$$

The influence of dz on the solution is shown in Figure 3.

The step size d$z=10^{-4}$ m is selected according to this result. By the next minimalisation, the solution is no longer influenced significantly.

Solving Equation (2), Figures 4 and 5 show the temperature distribution in float glass for different beam profiles. The temperature is calculated by using

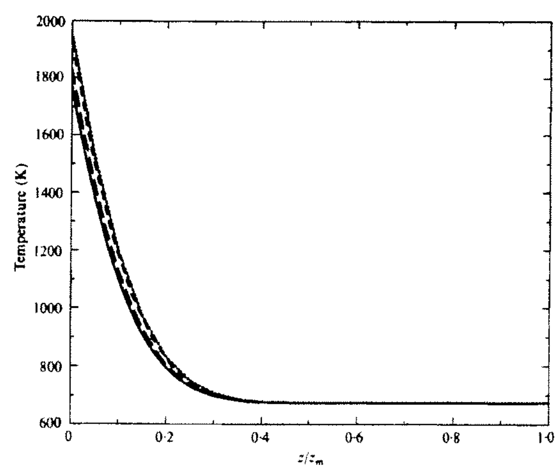

Figure 3. *Influence of step size dz on the solution of (2) ($I_0=300$ W/cm², t = 0·5 s, $T_0=673$ K, $T_{z_m}=T_0$, $-k(dT/dz)_0=I_0(1-R)$, k and c_p constant*
------ d$z=5\times10^{-4}$ m ——— d$z=1\times10^{-4}$ m
----- d$z=2\times10^{-4}$ m ——— d$z=5\times10^{-5}$ m

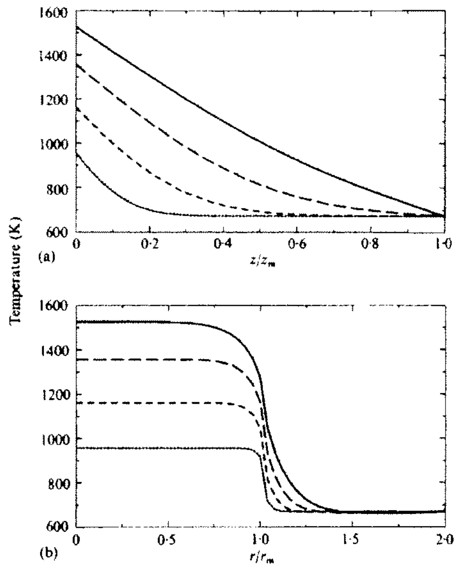

Figure 4. *Temperature profile for a rectangular intensity distribution ($I_0 = 142$ W/cm², $T_0 = 673$ K): (a) r = 0 and (b) z = 0*
.... $t = 0{\cdot}25$ s — — — $t = 2{\cdot}5$ s
- - - - - $t = 1$ s ——— $t = 5$ s

temperature dependent glass properties ($k = f(T)$ according to Equation (10), $c_p = f(T)$ according to Equation (12)) and considering radiation losses at the front side and losses equal to the flux at the rear side ($T_{z_m} = T_0$). The depth profile appears independent of the beam profile because the beam radius r_m is much larger than the thickness z_m. Therefore, the two dimensional problem can be replaced with a one dimensional solution.

The comparison of the results for different boundary conditions, temperature dependent, and temperature independent thermal properties is given in Figures 6, 7 and 8.

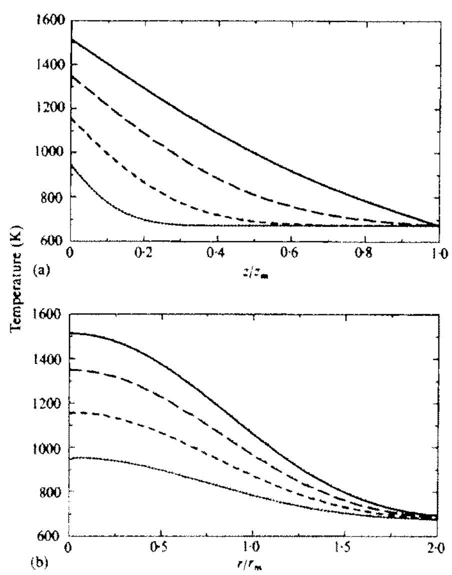

Figure 5. *Temperature profile for a Gaussian intensity distribution ($I_0 = 142$ W/cm², $T_0 = 673$ K): (a) r = 0 and (b) z = 0*
.... $t = 0{\cdot}25$ s — — — $t = 2{\cdot}5$ s
- - - - - $t = 1$ s ——— $t = 5$ s

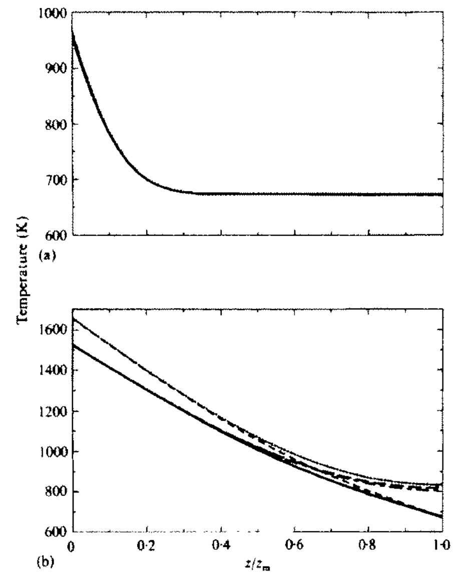

Figure 6. *Temperature distribution in float glass ($z_m = 4$ mm) for differing boundary conditions ($I_0 = 142$ W/cm², $T_0 = 673$ K): (a) t = 0·25 s and (b) t = 5 s*
- - - - - - case 1 — - · case 3 ——— case 5
- - - - - case 2 — — — case 4

Table 2. *Temperature distributions in float glass for different boundary conditions*

Case	*Front surface* $-k\left[\frac{\partial T}{\partial z}\right]_{z=0}$	*Back surface* $-k\left[\frac{\partial T}{\partial z}\right]_{z=z_m}$
1	$I(r)$	0
2	$I(r)$	$T_{z_m} = T_0$
3	$I(r) - \sigma\varepsilon(T^4_{z=0} - T^4_c)$	$\sigma\varepsilon(T^4_{z_m} - T^4_c)$
4	$I(r) - \sigma\varepsilon(T^4_{z=0} - T^4_c)$	0
5	$I(r) - \sigma\varepsilon(T^4_{z=0} - T^4_c)$	$T_{z_m} = T_0$

The influence of various boundary conditions is shown in Figure 6 and Table 2, neglecting convection losses, with $k = f(T)$ according to Equation (10), $c_p = f(T)$ according to Equation (12). It is obvious that different boundary conditions become important for long irradiation times, $t \geq 2$ s. Energy losses due to heat radiation at high temperatures lower the surface temperature at the hot irradiated front side ($z = 0$) drastically. At moderate temperatures, as observed at the back side, the radiation losses are not as significant as at higher front surface temperatures. In the experiments the boundary conditions at the rear side can be determined by the set up.

The influence of c_p on the temperature distribution is shown in Figure 7. Radiation losses at front and back surface are taken into account, with $k = f(T)$ according to Equation (10). The profile does not vary much with different dependences of c_p. The temperature dependence has only a minute influence.

Figure 8 shows the temperature profile varying the

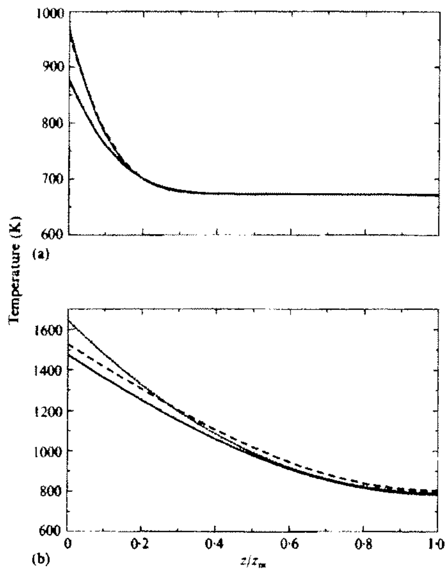

Figure 7. *Temperature distribution in float glass for differing specific heats ($I_0 = 142$ W/cm^2, $T_0 = 673$ K): (a) t = 0·25 s and (b) t = 5 s*
- - - - - - c_p = const ——— $c_p = f(T)$, with jump at T_g
– – – – – $c_p = f(T)$

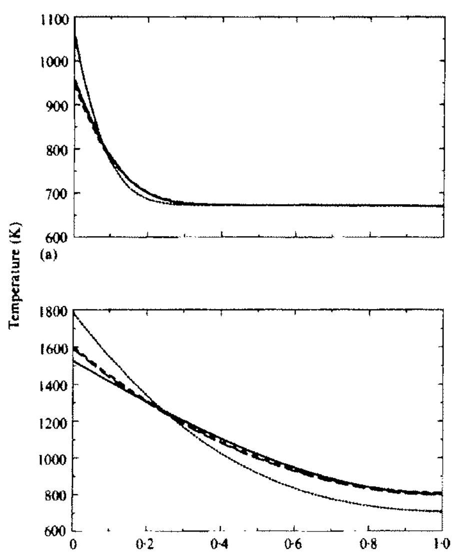

Figure 8. *Temperature distribution in float glass for differing thermal conductivities ($I_0 = 142$ W/cm^2, $T_0 = 673$ K): (a) t = 0·25 s and (b) t = 5 s*
- - - - - - $k = k_1$ — — — $k = f(T)$
– – – – – $k = k_2$ ——— $k = k(T^4)$

thermal conductivity. Radiation losses at both surfaces are taken into account, with $c_p = f(T)$ according to Equation (12). The heat transfer by photons has a significant influence on the temperature profile compared to the rather small effect of the phonon conductivity. At high temperatures the thermal conductivity becomes rather large considering additional heat transfer by radiation. Therefore, the temperature dependence is of great importance for long irradiation times. Photon conductivity enables a rather quick flux of heat and therefore a more even temperature distribution within the glass. For future research, it is therefore necessary to use the more precise temperature dependence of heat conductivity (the dependence in this work was an extrapolation for temperatures above 600°C). It follows, that the sample thickness may be of great importance. For thin samples ($z_m \rightarrow 0$) the effective glass conductivity is near the real conductivity, i.e. independent of temperature above about 600°C. As thickness increases, the radiation heat transfer mechanism is of increasing importance. For an infinite thickness, radiation accounts for nearly 100% of the heat transfer and the temperature dependence is very strong. The comparison of experimental results with the model solutions should solve this problem.

Conclusion

In the case of a laser beam with large radius compared to the material thickness the one dimensional solution of the heat conduction equation is satisfactory. The results show that radiation losses at the front side, taking the temperature dependence of the thermal conductivity into account, have a significant influence on the temperature. The temperature dependence of the glass properties k and c_p have a large influence on the temperature distribution in glass. The higher the thermal conductivity, the higher the specific heat of the material and the more even is the temperature distribution in the glass. For laser treatment, the consideration of energy losses due to radiation at the irradiated front side has the largest effect. A series of experiments with samples of different thickness must be carried out, with the surface temperature being monitored with an infrared pyrodetector. The influence of sample thickness on the heat conduction equation will be the subject of the next work.

References

1. Geith, A., Buerhop, C., Jaschek, R., Weißmann, R., Helebrant, A. & Bergmann, H. W. Polishing of lead crystal glass using cw CO_2 lasers. *Fourth Eur. Conf. on Laser Treatment of Materials (ECLAT 92)*, 1992, Pp. 521–6.
2. Carslaw, H. S. & Jaeger, J. C. *Conduction of heat in solids*. Second edition. 1959. Clarendon Press, Oxford.
3. Zscherpe, G. Wärmeleitmodelle zur Laserbestrahlung von Werkstoffen. *Feingerätetechnik*, 1981, **30** (8), 365.
4. Geissler, E. & Bergmann, H. W. 3D temperature fields in laser transformation hardening. Part 2. Nonstationary fields. In *European scientific laser workshop on mathematical simulation*. 1989, Sprechsaal, Lisbon.
5. Geotti-Bianchini, F., De Riu, L., Gagliardi, G., Guglielmi, M. & Pantano, C. G. New interpretation of the infrared reflectance spectra of SiO_2 rich films on soda–lime glass. *Glastech. Ber.*, 1991, **64** (8), 205–17.
6. Buerhop, C., Blumenthal, B., Weißmann, R., Lutz, N. & Biermann, S. Glass surface treatment with excimer and CO_2 lasers. *Appl. Surf. Sci.*, 1990, **46**, 430–4.
7. Ammar, M. M., Gharib, S. A., Halawa, M. M., El-Batal, H. A. & El-Badry, K. Thermal conductivity of silicate and borate glasses. *J. Am. Ceram. Soc.*, 1983, **66**, C76–77.
8. Moore, H. & Sharp, D. E. Note on calculation of effect of temperature and composition of specific heat of glass. *J. Am. Ceram. Soc.*, 1958, **41**, 461–3.